RSC Advances

ROYAL SOCIETY OF CHEMISTRY

www.rsc.org/advances

ChemComm

RSCPublishing

ARTICLE

Exfoliated MoS_2 supported Au–Pd bimetallic nanoparticles with core-shell structures and superior peroxidase-like activities

Zhen Sun,[a] Qingshan Zhao,[a] Guanghui Zhang,[a] Yang Li,[a] Guoliang Zhang,[a] Fengbao Zhang[a] and Xiaobin Fan[a]*

Cite this: DOI: 10.1039/xoxxoooooox

Received ooth January 2012,
Accepted ooth January 2012

DOI: 10.1039/xoxxoooooox

www.rsc.org/

Au–Pd bimetallic nanoparticles (NPs) with core-shell structures have been successfully anchored on chemical exfoliated MoS_2 (Au–Pd/MoS_2) through a facile co-reduction method at room temperature. The Au–Pd/MoS_2 hybrids were characterized by X-ray diffraction (XRD), scanning electronic microscopy (SEM), high-resolution transmission electron microscopy (HRTEM), energy dispersive X-ray spectroscopy (EDX) and X-ray photoelectron spectroscopy (XPS). The pristine MoS_2 nanosheets exhibit some peroxidase-like activity for the oxidation of 3,3,5,5-tetramethylbenzidine (TMB), and its catalytic activity is significantly enhanced by the deposition of Au–Pd NPs. Systematic study revealed that Au–Pd NPs with a mass ratio of 1:2 on MoS_2 ($Au_{1.0}Pd_{2.0}/MoS_2$) showed the highest catalytic activity compared with other counterparts. This excellent performance of the $Au_{1.0}Pd_{2.0}/MoS_2$ hybrids should be ascribed to not only the intrinsic catalytic activity of MoS_2, but also the complicated metal–metal and metal–support interactions.

Introduction

Transition metal dichalcogenides (TMDs), especially the exfoliated MoS_2 have attracted great interest due to its unique physical and chemical properties. These features render MoS_2 wide applications ranging from electronic devices, transistors, energy storage devices to catalysis.[1-4] Recently, MoS_2 has been demonstrated to be a perfect material to construct functional hybrid nano-composites.[5-7] In particular, many monometallic nanoparticles (NPs), such as Cu,[8] Ni,[9, 10] Ag,[11, 12] Au,[13, 14] Pt and Pd[15, 16] NPs have been successfully dispersed on MoS_2 aiming to achieve enhanced performance in various applications. So far, however, few studies reach MoS_2 supported bimetallic NPs hybrids, though the advantages of adding the second metal have been clearly demonstrated on other supports.[17-20] Normally, adding the second metal can alter the electronic and geometrical properties of the bimetal NPs, which may have a positive effect on their catalytic activity and stability.[21] For example, Au–Pd nanohybrids are well-known for their higher activities towards various reactions, such as CO oxidation,[22] hydrogen production,[23] solvent free oxidation of primary alcohols to aldehydes,[24] direct synthesis of H_2O_2[25] and selective oxidation of methanol to methyl formate[26]. Nevertheless, corresponding studies on MoS_2 have been hampered by lacking of effective methods to immobilize the bimetallic NPs. Most recently, Ma's group have reported the improved hydrazine oxidation activities using Ni–Fe alloy supported on MoS_2 and functionalized MoS_2 nanosheets by electrodeposition and electroplating approach, respectively.[27, 28] However, developing a more simple method to disperse the bimetallic NPs with different heterostructures on MoS_2 is still a challenge.

In this paper, we report a facile co-reduction method to prepare MoS_2 supported Au–Pd NPs with core-shell structure (Au–Pd/MoS_2) and the obtained hybrids have been applied in the oxidation of 3,3,5,5-tetramethylbenzidine (TMB) (Scheme 1). By simultaneous reduction of $HAuCl_4$ and K_2PdCl_4 mixture with tannic acid at room temperature, Au–Pd NPs can be successfully dispersed on the MoS_2 support. Comparing studies revealed that Au–Pd/MoS_2 showed superior peroxidase-like performance towards the oxidation of TMB in the presence of H_2O_2. The influence of Au/Pd mass ratio on the catalytic was also systematic investigated.

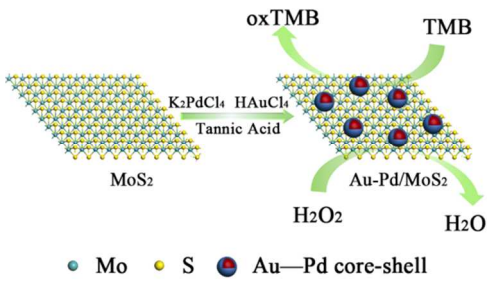

Scheme 1 Illustration for the preparation of Au–Pd/MoS_2 hybrids and its catalytic oxidation of TMB.

Experimental

Materials

Commercially available molybdenum sulphide (MoS_2) powder (<2 μm, 99%), n-butylithium (n-BuLi, 1.6 M hexane solution), $HAuCl_4•3H_2O$, K_2PdCl_4, TMB (3, 3, 5, 5-tetramethylbenzidine) (98%) are all analytical grade, purchased from Aladdin Chemistry Co., Ltd., Shanghai, China. Tannic acid was provided by J&K Scientific Ltd., Beijing, China. In addition, the deionized water was used in all experiments. All the chemicals were used as supplied without further purification.

Characterization

The as-prepared MoS_2 nanosheets and Au–Pd/MoS_2 hybrids were characterized by X-ray diffraction (XRD) (Bruker-Nonius D8 FOCUS diffractometer), scanning electron microscope (SEM) (Hitachi S-4800), high-resolution transmission electron microscopy (HRTEM) (Philips Tecnai G2 F20), X-ray photoelectron spectroscopy (XPS) (Perkin-Elmer, PHI 1600 spectrometer), energy dispersive X-ray spectroscopy (EDX) (Philips Tecnai G2 F20 & Hitachi S-4800) and inductively coupled plasma optical emission spectroscopy (ICP-OES, Vista-MPX). Ultraviolet-visible (UV-vis) absorption spectra were monitored by UV-2802H during the reaction.

Synthesis of Au–Pd /MoS_2 hybrids

MoS_2 nanosheets were obtained by chemically exfoliated method following the procedure reported befor.[29, 30] In addition, the as-made MoS_2 nanosheets were purified by using exhaustive dialysis.

Catalysts with 23wt% of Au–Pd NPs on MoS_2 were prepared by co-reduction method. 7.67wt%Au–15.33wt%Pd/MoS_2 ($Au_{1.0}Pd_{2.0}/MoS_2$)was prepared by the following procedure: 100 mL MoS_2 (0.1 mg mL^{-1}) aqueous solution was centrifuged at 6800 g for 20 min. The supernatant was removed, and the precipitate was re-dispersed in 50 mL aqueous solution containing 0.025 mmol tannic acid. Then 0.25 mL of 0.02 M $HAuCl_4$ aqueous solution and 0.94 mL of 0.02 M K_2PdCl_4 aqueous solution were added with magnetic stirring. The color of the solution turned from dark brown to black. After 1 h, the product was extensively washed with ethanol and deionized water for purification. Catalysts with other Au/Pd ratios were prepared in a similar method but using different quantities of $HAuCl_4$ and K_2PdCl_4 aqueous solutions. The Au–Pd NPs were also prepared for control experiments in the same method without adding MoS_2.

Catalytic oxidation of TMB by Au-Pd/MoS_2

The oxidation reaction of TMB was carried out to testify the catalytic activity of the as-prepared hybrids. 0.2 mL TMB (2.88 mg mL^{-1}), 0.06 mL Au–Pd/MoS_2 hybrids (1.67 mg mL^{-1}) and 50 μL H_2O_2 (30%) were added into 2.7 mL sodium acetate buffer solution (pH 3.6) at room temperature. The reaction was carried out in a quartz cuvette. Reaction time and spectra evolutions from 500 to 800 nm were recorded once H_2O_2 was added. Evolution of absorbance spectra over time was monitored after the same interval. The other catalysts were also utilized under the same reaction condition.

Results and discussions

Synthesis of Au–Pd/MoS_2 hybrids

The exfoliated nature of the MoS_2 nanosheets was investigated by the X-ray diffraction (XRD) (Fig. 1). Compared with the bulk form of MoS_2 (black line), the exfoliated MoS_2 (blue line) displays three broad diffraction peaks, which correspond to the (002), (100) and (110) planes of MoS_2 (JCPDS 37-1492). Note that the absence of (103) and (105) peaks provides a direct evidence for its exfoliated structure.[31, 32] In addition, different from the exfoliated MoS_2 in suspension, the dried sample retains a small but broadening (002) peak, attributing to the random re-stacking of exfoliated MoS_2. This hypothesis is not only supported by the asymmetric broadening of the (100) peaks, but also consists with later scanning electron microscope (SEM) (Fig. 2) observation. After the co-reduction of $HAuCl_4$ and K_2PdCl_4 in the present of exfoliated MoS_2, two obvious peaks appear at 2θ = 38.68° , 44.71° . The green and brown lines correspond to the characteristic peaks (111), (200) and (220) of Au and Pd respectively (JCPDS 04-0784, 46-1043). The shift of (110) peak may be caused by employing tannic acid, leading to the change in lattice parameters.

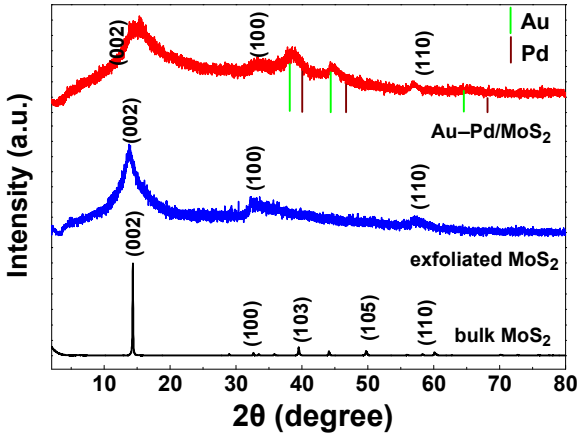

Fig. 1 XRD patterns of pristine MoS_2 powder, exfoliated MoS_2 nanosheets and Au–Pd/MoS_2 hybrids (from bottom to top). Note that the change of (002) should be ascribed to relatively weak signal and concave sample surface.

The surface morphological study was first performed by SEM. As shown in Fig. 2a, re-stacking layers of sheet-like exfoliated MoS_2 with crumpling features can be clearly observed. In Fig. 2b, the layered MoS_2 serves as a support heavily decorated with NPs. The detailed structure and component of the supported NPs were further detected by transmission electron microscopy (TEM) (Fig. 3) and energy dispersive X-ray spectroscopy (EDX) analysis (Fig. S1, see ESI).

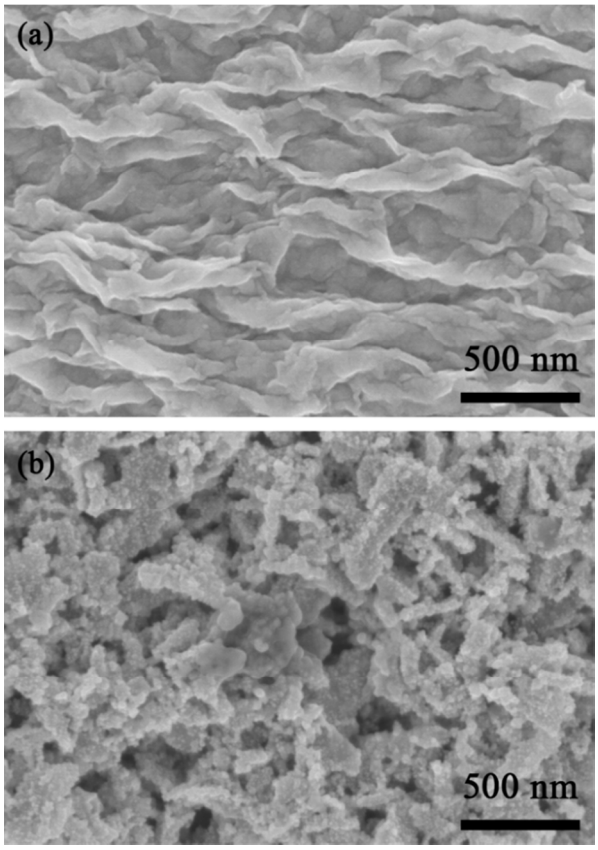

Fig. 2 SEM images of (a) MoS_2 naosheets and (b) Au–Pd/MoS_2 hybrids

Consistent with the SEM results, typical TEM image of the obtained MoS_2 nanosheets (Fig. 3a) shows rough surfaces. Actually, re-stacking of small MoS_2 nanosheets and clear folded edges can be also occasionally observed. HRTEM image (Fig. 3b) reveals that the MoS_2 nanosheets consist of the honeycomb and hexagonal lattices with a random distribution on the plane, indicating the heterogeneous phase structure that coexists of 2H and 1T phases.[33] It is further confirmed by XPS spectra of Mo and S (Fig. 4a and b). The result is in accordance with previous reports on chemical exfoliated MoS_2 and can be explained by the change in the metal coordination during the Li intercalation process.[29, 34, 35] In addition, lattice spacing of 0.27 nm corresponding to the (100) lattice plane of MoS_2 can be clearly observed.[36, 37] A typical TEM image of Au–Pd/MoS_2 hybrid is shown in Fig. 3c. The NPs are homogeneously distributed on the entire surface of the MoS_2 support. The sizes of NPs are in the range of 5–8 nm, with an average size of 6.68 nm, as reflected by the size distribution in Fig. 3e. Typical magnified image in Fig. 3d shows clear different contrast in core and the outer surface, indicating the formation of core-shell structure. A close look in core shows the typical lattice of gold with a d-spacing of 0.235 nm, corresponding to the (111) planes of face-centered cubic (fcc) Au. While the d-spacing in the shell region is 0.225 nm, representative to the (111) planes of fcc Pd.[38, 39] Compositional line profile (Fig. 3f) reveals that the Au are mainly located in the core while the Pd are concentrated in the shell region. These results confirm the formation of bimetallic Au–Pd NPs with core-shell structure on the exfoliated MoS_2 support.

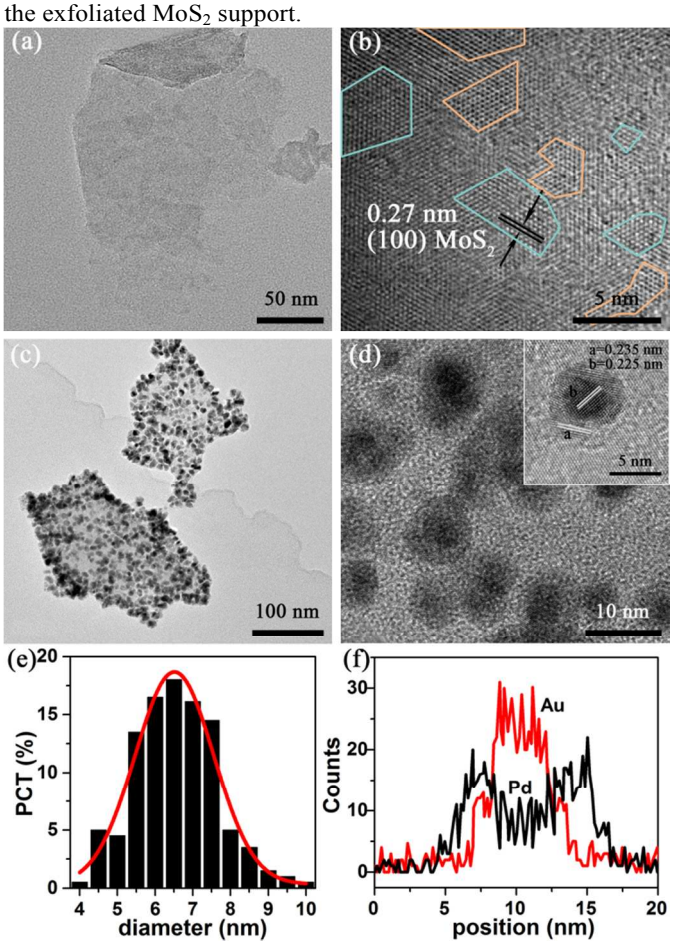

Fig. 3 (a) TEM and (b) HRTEM image of exfoliated MoS_2 nanosheet; (c) TEM and (d) HRTEM image (inset, the adjacent lattice fringes of Au–Pd NPs) of a typical Au–Pd/MoS_2 hybrid; (e) size distribution of the NPs and (f) cross-sectional compositional line profiles of one NP (the red and black lines represent the Au and Pd element, respectively).

X-ray photoelectron spectroscopy (XPS) was further employed to determine the component of the prepared samples. Mo, S, Au and Pd signals can be clearly observed in the full range of XPS spectra (Fig. S2, see ESI). The deconvolution of Mo 3d spectra in Fig 2a reveals the 1T components at 228.4 eV and 231.6 eV.[29, 40] These positions are shifted to lower binding energy with respect to the 2H MoS_2. Sub-peaks at 235.5 eV and 232.4 eV are also observed, representing Mo $3d_{3/2}$ and Mo $3d_{5/2}$, respectively, indicating the presence of MoO_3,[41] which might arise from surface oxidization. Similarly, in Fig. 2b, the binding energies of S $2p_{1/2}$ and S $2p_{3/2}$ peaks for 2H MoS_2 are located at 163.3 eV and 161.9 eV. Doublet peaks corresponding to S $2p_{1/2}$ and S $2p_{3/2}$ for 1T MoS_2 are at around 162.3 eV and 161.3 eV, respectively.[29] A small peak at 168.7 eV is assigned to sulfur oxide,[15] which may be introduced during the sample preparation. Moreover, the relative peak intensity of S $2p_{3/2}$ and S $2p_{1/2}$ is obviously increased after the co-reduction process. These changes could be attributed to the interaction between the NPs and the support. Fig. 4c and d provide the binding energies of Au and Pd, respectively. The

peaks for Au $4f_{5/2}$ and Au $4f_{7/2}$ located at about 87.5 eV and 83.8 eV, indicating that Au is present in the zero-valent metallic state.[42] In line with other reports,[18, 43] the value is slightly lower than those of bulk metallic gold[44] (87.7 eV for Au $4f_{5/2}$, 84.0 eV for Au $4f_{7/2}$).Whereas the peaks of Pd $3d_{3/2}$ and Pd $3d_{5/2}$ are 340.7 eV and 335.4 eV,[45] respectively, which are slightly higher than those of the bulk counterpart. The negative shift of the Au 4f peak and the positive shift of the Pd peak suggest a charge transfer from Pd to Au atoms,[46] which indicates a strong synergism between Au and Pd in the Au–Pd/MoS_2 hybrid.[26]

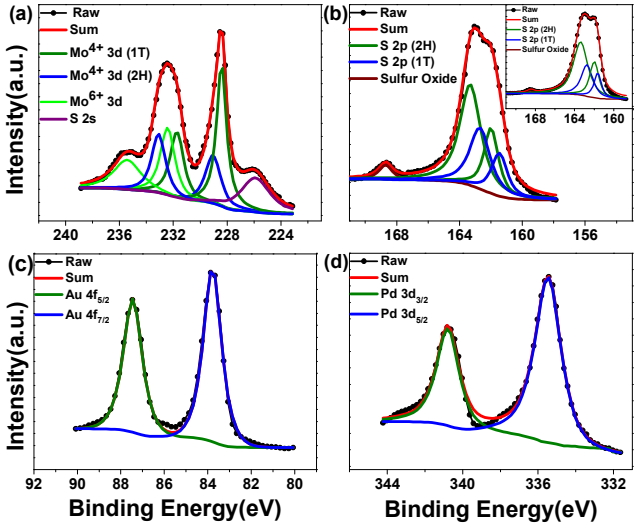

Fig. 4 (a) Mo 3d XPS spectra of Au–Pd/MoS_2, (b) S 2p XPS spectra of Au–Pd/MoS_2, (c) Au 4f and (d) Pd 3d XPS spectrum of Au–Pd/MoS_2. Inset in (b) is S 2p spectra of MoS_2.

Catalytic reaction

TMB oxidation was carried out (pH 3.6) to investigate the catalytic ability of the prepared Au–Pd/MoS_2 hybrids. UV spectroscopy was employed in this study to evaluate the peroxidase activity of the Au–Pd/MoS_2. In a typical TMB oxidation process, the color of the transparent substrate (TMB) will turn blue after the addition of catalysts and H_2O_2.[47] As shown in Fig. 5a, when Au–Pd/MoS_2 is used as catalyst, the absorbance quickly increases at 652 nm with time increasing. At the same time, blue color can be clearly seen in the quartz cuvette (Fig. 5b).

In order to identify the interaction between the layered MoS_2 and the Au–Pd NPs, control experiments were also conducted. As shown in Fig. 5c, in the absence of catalyst, hardly any absorbance could be observed in the measured range. Although both MoS_2 and the unsupported Au–Pd NPs exhibit low activities, the Au–Pd/MoS_2 hybrids show an outstanding performance, suggesting a synergistic effect between the Au–Pd NPs and MoS_2 support. Furthermore, a series of catalysts with different Au/Pd mass ratios were also synthesized to systematically investigate their catalytic activities. The results are shown in Fig. 5d. Generally, the catalytic rates of Pd–rich catalysts are superior to those of Au–rich catalysts. This assumption is also supported by the fact that the Au/MoS_2 hybrid is significantly less active than the Pd/MoS_2 (Fig. S3, see ESI). The activities are enhanced by increasing the Pd content in the bimetallic NPs. It is worth noting that a steady increase of the rate is observed up to $Au_{1.0}Pd_{2.0}$ and a drastic decrease occurs for the $Au_{1.0}Pd_{3.0}$ sample. This result suggests that the composition exerts a great influence on the activity. In addition, the $Au_{1.0}Pd_{2.0}$/MoS_2 hybrids possess high catalytic activities in the pH range of 3.0 to 4.6, and the optimal pH value is 3.6 (Fig. S3, see ESI). Moreover, XPS analysis reveals that the catalysts are oxidized after the catalytic reactions (Fig. S4, see ESI).

We believe that the enhanced performance of the $Au_{1.0}Pd_{2.0}$/MoS_2 hybrid is not only due to the intrinsic catalytic activity of MoS_2 and its two-dimensional structure, but also the strong interaction of metal–metal and metal–support. In brief, the MoS_2 nanosheets with a huge surface area provide plenty of nucleation sites for the growth of the Au–Pd NPs, avoiding their aggregation.[16] In addition, its two-dimensional structure facilitates the mass transfer during the reaction process, as the substrates and products can easily access and leave the catalytic active sites. On the other hand, with an appropriately lowered d-band center,[48, 49] Au–Pd NPs with an optimal composition and core-shell structure will increase the surface charge heterogeneity, which in turn changes their interaction with the reactants molecules.[50, 51] Moreover, the metal-support interaction[52] may also promote the electron transfer from the Au–Pd NPs to the MoS_2 support, reducing the activation energy. All these factors come together to endow the hybrids superior peroxidase-like activities.

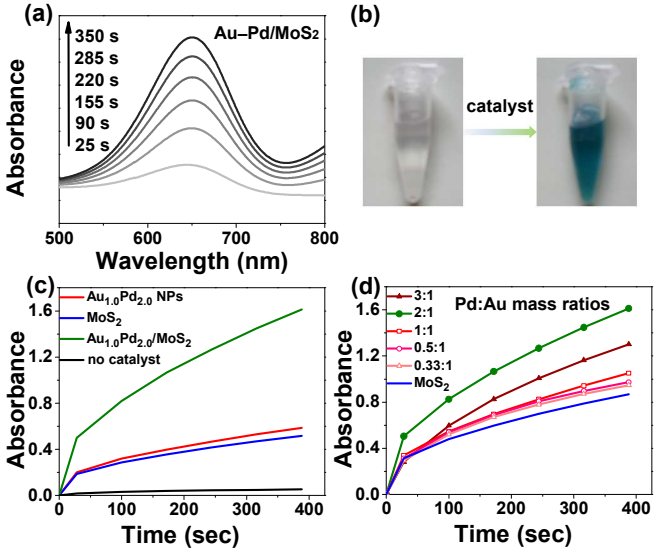

Fig. 5 The evolutions of absorbance spectra (a) and colour evolution (b) of TMB oxidation over time in the presence of Au–Pd/MoS_2 hybrid (pH 3.6), (c) Time-dependent absorbance changes at 652 nm using NPs and substrate (the amount of the catalysts is calculated on the basis of ICP results, Table S1,see ESI), (d) Time-dependent absorbance changes at 652 nm using Au–Pd/MoS_2 hybrids with different Au/Pd mass ratios.

Conclusions

In conclusion, we demonstrate a facile co-reduction method to immobilize Au–Pd NPs with core-sell structure on exfoliated MoS_2 nanosheets for the first time. Notably, the prepared Au–Pd/MoS_2 hybrid exhibits superior peroxidase-like performance towards the oxidation of TMB. We also found that the hybrid with Au/Pd mass ratio of 1:2 ($Au_{1.0}Pd_{2.0}/MoS_2$) shows the highest catalytic activity due to the clear synergic effect between the Au–Pd NPs and MoS_2 support. The advantages of the hybrids also lie in the fact that the Au cores can minimize the use of more expensive Pd precursors, reducing the cost of the catalyst. This strategy may be readily applied to prepare other exfoliated TMDs supported bimetallic nanoparticles with unique core-shell structures and excellent catalytic abilities.

Acknowledgements

This study was supported by the National Natural Science Funds for Excellent Young Scholars (No.21222608), Research Fund of the National Natural Science Foundation of China (No.21106099), Foundation for the Author of National Excellent Doctoral Dissertation of China (No. 201251), and the Programme of Introducing Talents of Discipline to Universities (No. B06006).

Notes and references

[a] State Key Laboratory of Chemical Engineering, School of Chemical Engineering & Technology, Collaborative Innovation Center of Chemical Science and Engineering, Tianjin University, Tianjin, 300072, China. E-mail: xiaobinfan@tju.edu.cn; Fax: +86 22-27890090; Tel: +86 22-27890090

† Electronic Supplementary Information (ESI) available: [catalysts characterization and additional results]. See DOI: 10.1039/b000000x/

1 Xu, M., Liang, T., Shi, M. and Chen, H., *Chem. Rev.*, 2013, **113**, 3766.
2 Chhowalla, M., Shin, H. S., Eda, G., Li, L.-J., Loh, K. P. and Zhang, H., *Nat. Chem.*, 2013, **5**, 263.
3 Rao, C. N. R., Ramakrishna Matte, H. S. S. and Maitra, U., *Angew. Chem. Int. Ed.*, 2013, **52**, 13162.
4 Butler, S. Z., Hollen, S. M., Cao, L., Cui, Y., Gupta, J. A., Gutiérrez, H. R., Heinz, T. F., Hong, S. S., Huang, J., Ismach, A. F., Johnston-Halperin, E., Kuno, M., Plashnitsa, V. V., Robinson, R. D., Ruoff, R. S., Salahuddin, S., Shan, J., Shi, L., Spencer, M. G., Terrones, M., Windl, W. and Goldberger, J. E., *ACS Nano*, 2013, **7**, 2898.
5 Yu, L., Lee, Y.-H., Ling, X., Santos, E. J. G., Shin, Y. C., Lin, Y., Dubey, M., Kaxiras, E., Kong, J., Wang, H. and Palacios, T., *Nano Lett.*, 2014, **14**, 3055.
6 J. Ollivier, P., E. Mallouk, T., J. Ollivier, P., I. Kovtyukhova, N. and W. Keller, S., *Chem. Commun.*, 1998, 1563.
7 Chiu, M.-H., Li, M.-Y., Zhang, W., Hsu, W.-T., Chang, W.-H., Terrones, M., Terrones, H. and Li, L.-J., *ACS Nano*, 2014, **8**, 9649.
8 Huang, J., Dong, Z., Li, Y., Li, J., Tang, W., Yang, H., Wang, J., Bao, Y., Jin, J. and Li, R., *Mater. Res. Bull.*, 2013, **48**, 4544.
9 Huang, J., He, Y., Jin, J., Li, Y., Dong, Z. and Li, R., *Electrochim. Acta*, 2014, **136**, 41.
10 Cheng, F. Y., Chen, J. and Gou, X. L., *Adv. Mater.*, 2006, **18**, 2561.
11 Xia, X., Zheng, Z., Zhang, Y., Zhao, X. and Wang, C., *Sens. Actuators, B: Chemical*, 2014, **192**, 42.
12 Yang, L., Zhong, D., Zhang, J., Yan, Z., Ge, S., Du, P., Jiang, J., Sun, D., Wu, X., Fan, Z., Dayeh, S. A. and Xiang, B., *ACS Nano*, 2014, **8**, 6979.
13 Yin, Z., Chen, B., Bosman, M., Cao, X., Chen, J., Zheng, B. and Zhang, H., *Small*, 2014, **10**, 3537.
14 Kim, J., Byun, S., Smith, A. J., Yu, J. and Huang, J., *J. Phys. Chem. Lett.*, 2013, **4**, 1227.
15 Yuwen, L., Xu, F., Xue, B., Luo, Z., Zhang, Q., Bao, B., Su, S., Weng, L., Huang, W. and Wang, L., *Nanoscale*, 2014, **6**, 5762.
16 Huang, X., Zeng, Z., Bao, S., Wang, M., Qi, X., Fan, Z. and Zhang, H., *Nat. Commun.*, 2013, **4**, 1444.
17 Qi, J., Lv, W., Zhang, G., Li, Y., Zhang, G., Zhang, F. and Fan, X., *Nanoscale*, 2013, **5**, 6275.
18 Ouyang, L., Da, G.-j., Tian, P.-f., Chen, T.-y., Liang, G.-d., Xu, J. and Han, Y.-F., *J. Catal.*, 2014, **311**, 129.
19 Long, J., Liu, H., Wu, S., Liao, S. and Li, Y., *ACS Catal.*, 2013, **3**, 647.
20 Sarina, S., Bai, S., Huang, Y., Chen, C., Jia, J., Jaatinen, E., Ayoko, G. A., Bao, Z. and Zhu, H., *Green Chem.*, 2014, **16**, 331.
21 Sankar, M., Dimitratos, N., Miedziak, P. J., Wells, P. P., Kiely, C. J. and Hutchings, G. J., *Chem. Soc. Rev.*, 2012, **41**, 8099.
22 Cheng, D., Xu, H. and Fortunelli, A., *J. Catal.*, 2014, **314**, 47.
23 Su, R., Tiruvalam, R., Logsdail, A. J., He, Q., Downing, C. A., Jensen, M. T., Dimitratos, N., Kesavan, L., Wells, P. P., Bechstein, R., Jensen, H. H., Wendt, S., Catlow, C. R. A., Kiely, C. J., Hutchings, G. J. and Besenbacher, F., *ACS Nano*, 2014, **8**, 3490.
24 Enache, D. I., Edwards, J. K., Landon, P., Solsona-Espriu, B., Carley, A. F., Herzing, A. A., Watanabe, M., Kiely, C. J., Knight, D. W. and Hutchings, G. J., *Science*, 2006, **311**, 362.
25 Edwards, J. K., Solsona, B. E., Landon, P., Carley, A. F., Herzing, A., Kiely, C. J. and Hutchings, G. J., *J. Catal.*, 2005, **236**, 69.
26 Wang, R., Wu, Z., Chen, C., Qin, Z., Zhu, H., Wang, G., Wang, H., Wu, C., Dong, W., Fan, W. and Wang, J., *Chem. Commun.*, 2013, **49**, 8250.
27 Zhong, X., Yang, H., Guo, S., Li, S., Gou, G., Niu, Z., Dong, Z., Lei, Y., Jin, J., Li, R. and Ma, J., *J. Mater. Chem.*, 2012, **22**, 13925.
28 Li, J., Tang, W., Yang, H., Dong, Z., Huang, J., Li, S., Wang, J., Jin, J. and Ma, J., *RSC Adv.*, 2014, **4**, 1988.
29 Eda, G., Yamaguchi, H., Voiry, D., Fujita, T., Chen, M. and Chhowalla, M., *Nano Lett.*, 2011, **11**, 5111.
30 Joensen, P., Frindt, R. F. and Morrison, S. R., *Mater. Res. Bull.*, 1986, **21**, 457.
31 Joensen, P., Crozier, E. D., Alberding, N. and Frindt, R. F., *J. Phys. C: Solid State Phys.*, 1987, **20**, 4043.
32 Yin, Z., Li, H., Li, H., Jiang, L., Shi, Y., Sun, Y., Lu, G., Zhang, Q., Chen, X. and Zhang, H., *ACS Nano*, 2011, **6**, 74.
33 Eda, G., Fujita, T., Yamaguchi, H., Voiry, D., Chen, M. and Chhowalla, M., *ACS Nano*, 2012, **6**, 7311.
34 Dungey, K. E., Curtis, M. D. and Penner-Hahn, J. E., *Chem. Mater.*, 1998, **10**, 2152.
35 Lukowski, M. A., Daniel, A. S., Meng, F., Forticaux, A., Li, L. and Jin, S., *J. Am. Chem. Soc.*, 2013, **135**, 10274.
36 Liu, B., Chen, L., Liu, G., Abbas, A. N., Fathi, M. and Zhou, C., *ACS Nano*, 2014, **8**, 5304.
37 Wang, Y., Ou, J. Z., Balendhran, S., Chrimes, A. F., Mortazavi, M., Yao, D. D., Field, M. R., Latham, K., Bansal, V., Friend, J. R., Zhuiykov, S., Medhekar, N. V., Strano, M. S. and Kalantar-zadeh, K., *ACS Nano*, 2013, **7**, 10083.
38 Tsen, S. C. Y., Crozier, P. A. and Liu, J., *Ultramicroscopy*, 2003, **98**, 63.

39 Dimitratos, N., Villa, A., Wang, D., Porta, F., Su, D. and Prati, L., *J. Catal.*, 2006, **244**, 113.
40 Lee, J. H., Jang, W. S., Han, S. W. and Baik, H. K., *Langmuir*, 2014, **30**, 9866.
41 Park, W., Baik, J., Kim, T.-Y., Cho, K., Hong, W.-K., Shin, H.-J. and Lee, T., *ACS Nano*, 2014, **8**, 4961.
42 Brust, M., Walker, M., Bethell, D., Schiffrin, D. J. and Whyman, R., *J. Chem. Soc., Chem. Commun.*, 1994, 801.
43 Marx, S. and Baiker, A., *J Phys. Chem. C*, 2009, **113**, 6191.
44 Bulushev, D. A., Yuranov, I., Suvorova, E. I., Buffat, P. A. and Kiwi-Minsker, L., *J. Catal.*, 2004, **224**, 8.
45 Zhou, W. P., Lewera, A., Larsen, R., Masel, R. I., Bagus, P. S. and Wieckowski, A., *J. Phys. Chem. B*, 2006, **110**, 13393.
46 Feng, Y., Yin, H., Gao, D., Wang, A., Shen, L. and Meng, M., *J. Catal.*, 2014, **316**, 67.
47 Shi, W., Wang, Q., Long, Y., Cheng, Z., Chen, S., Zheng, H. and Huang, Y., *Chem. Commun.*, 2011, **47**, 6695.
48 Hu, S., Scudiero, L. and Ha, S., *Electrochem. Commun.*, 2014, **38**, 107.
49 Tang, W. and Henkelman, G., *J. Chem. Phys.*, 2009, **130**.
50 Jiang, H.-L. and Xu, Q., *J. Mater. Chem.*, 2011, **21**, 13705.
51 Wu, J., Li, P., Pan, Y.-T., Warren, S., Yin, X. and Yang, H., *Chem. Soc. Rev.*, 2012, **41**, 8066.
52 Liu, J., *ChemCatChem*, 2011, **3**, 934.

